Colloid Polym Sci (2011) 289:301–308
DOI 10.1007/s00396-010-2349-9

ORIGINAL CONTRIBUTION

Biodegradable star-shaped poly(ethylene glycol)-poly (β-amino ester) cationic pH/temperature-sensitive copolymer hydrogels

Cong Truc Huynh · Minh Khanh Nguyen · Dai Phu Huynh · Doo Sung Lee

Received: 3 September 2010 / Revised: 31 October 2010 / Accepted: 23 November 2010 / Published online: 14 December 2010

Abstract Biodegradable star-shaped copolymers comprised of four-arm poly(ethylene glycol) (4-arm PEG) and poly(β-amino ester) (PAE) were synthesized by conjugating PAE to 4-arm PEG. The synthesized copolymers were characterized by ^{1}H and ^{13}C NMR and gel permeation chromatography. The PAE showed pH/temperature-sensitive properties in an aqueous solution. The copolymer solutions (30 wt.%) showed a gel-to-sol phase transition as a function of temperature in the pH range 7.2–7.8. The gel window covers the physiological conditions (37 °C and pH 7.4) and can be controlled by varying the PAE block length, copolymer solution concentration and PEG molecular weight. After a subcutaneous injection of the copolymer solution into a SD rat, a gel formed rapidly in situ which remained for more than 2 weeks in the body. This copolymer is expected to be a potential candidate for biomedical applications.

Keywords Hydrogels · Poly(β-amino ester) · Star-shaped copolymer · pH/temperature-sensitive · Biodegradable

C. T. Huynh · M. K. Nguyen · D. P. Huynh · D. S. Lee (✉)
Theranostic Macromolecules Research Center,
Department of Polymer Science and Engineering,
Sungkyunkwan University,
Suwon, Gyeonggi-do 440-746, South Korea
e-mail: dslee@skku.edu

D. P. Huynh
National Key Laboratory of Polymer and Composite Materials,
Ho Chi Minh City University of Technology,
268 Ly Thuong Kiet, Dist. 10,
Ho Chi Minh City, Vietnam

Present Address:
M. K. Nguyen
Department of Biomedical Engineering,
Case Western Reverse University,
Cleveland, OH 44106, USA

Introduction

Stimuli-sensitive polymeric physical hydrogels have attracted considerable interest for biomedical applications, such as drugs/proteins delivery and tissue engineering, because of their biocompatibility and lack of chemical cross-links that allows ultimate excretion from the body [1–5]. Thermosensitive polymeric hydrogels using triblock copolymers, which are composed of hydrophilic poly(ethylene glycol) (PEG) and various hydrophobic blocks, such as poly(L-lactic acid) (PLLA-PEG-PLLA) [4], poly(lactide-co-glycolide) (PLGA-PEG-PLGA) [5, 6], poly(caprolactone) (PCL-PEG-PCL) [7], *N*-isopropylacrylamide and its derivative [8, 9], and poly (phosphazene) [10], can be used as an injectable system for drugs/proteins delivery and biomedical applications. The biocompatibility and injectability of these copolymers are the most important factors. However, the neutral property limits their applications in the delivery of ionic drugs/proteins.

Recently, hydrogels in response to dual stimuli, particularly pH and temperature, have become an important topic [11–20]. Cationic hydrogels bearing tertiary amine groups, which can bind to anionic drugs/proteins through ionic interactions, were introduced as excellent materials for drug delivery systems [11, 12]. Typical cationic hydrogels, such as poly(β-amino ester) (PAE) [11–13], poly(amidoamine) (PAA) [14–16], poly(amino urethane) (PAU) [20], poly (ethylene imine) [21], and poly(lysine) [22], have been used to deliver drug molecules, proteins, and genes.

The gelation behavior of polymeric hydrogels was strongly affected the polymer structures, particularly star-shaped structures [23–26]. Star-shaped thermosensitive copolymer hydrogels was first reported by Choi et al. [23]. Copolymers composed of hydrophilic eight-arm PEG as the inner block and poly(L-lactide) (PEG(-PLLA)$_8$) and PCL (PEG(-PCL)$_8$) as the outer blocks were used. The hydrophobic interactions

of the PLLA and PCL blocks led to gelation. Subsequently, the stereocomplex gelation of star-shaped PEG(-PLLA)$_8$ and PEG-poly(D-lactide) (PEG(-PDLA)$_8$) with the contribution of enantiomeric PLLA and PDLA segments was reported [24]. The star-shaped copolymer of PEG(-PLLA)$_8$ itself could not form a gel but its cholesterol end-capped exhibited a sol-to-gel transition [25]. The hydrophobic interaction of cholesterol groups triggered gelation. Recently, our group reported the pH/temperature-sensitive copolymer hydrogels using star-shaped PEG(-PAU)$_4$ [26]. The interaction between the hydrophobic deionized non-biodegradable PAU blocks and the 4-arm PEG crosslinker promoted gelation. However, no biodegradable star-shaped polymeric hydrogels that are sensitive to both pH and temperature have been reported.

The biodegradable property of materials is a key factor for using in biomedical field. In this study, therefore, we synthesized a series of novel biodegradable pH/temperature-sensitive star-shaped copolymer hydrogels, a potential candidate for biomedical applications. The copolymer composed of 4-arm poly(ethylene glycol) and poly(β-amino ester) was synthesized and characterized by ^{1}H and ^{13}C NMR and gel permeation chromatography (GPC). The sol–gel properties and affecting factors were examined. The gelation and gel stability in vivo were also investigated.

Experimental

Materials

Poly(ethylene glycol)s (4-arm PEG) were purchased from ID Biochem, Inc. (Seoul, Korea) and used as received. Acryloyl chloride (AC), anhydrous toluene, anhydrous dichloromethane (DCM), triethylamine (TEA), 4,4′-trimethylene dipiperidine (TMDP), 1,6-hexanediol diacrylate (HDDA), and phosphate buffer saline (PBS) were obtained from Sigma-Aldrich (St. Louis, MO, USA) and used as received. Hydrochloric acid (HCl), sodium hydroxide (NaOH), tetrahydrofuran (THF), and diethyl ether were all products from Samchun Co. (Seoul, Korea). All other reagents were of analytical grade and used without further purification.

Synthesis of PEG(-PAE)$_4$ copolymers

Star-shaped PEG(-PAE)$_4$ block copolymers were synthesized by conjugating PAE to acrylated 4-arm PEG (4-arm PEG-A).

Synthesis of 4-arm PEG-A

Four-arm PEG-A was synthesized by coupling AC to the hydroxyl groups at the end of PEG in toluene in the presence of TEA as a catalyst (Scheme 1). The synthetic

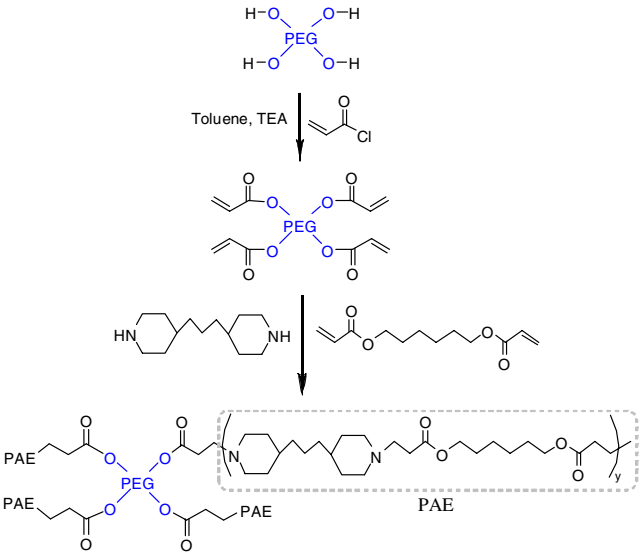

Scheme 1 Synthesis route of the PEG(-PAE)$_4$ copolymers

processing of 4-arm PEG-A (M_n=10,000) was as follows: PEG (1 mmol) was dried for 2 h under vacuum at 100 °C in a 250-mL two-neck round-bottom flask equipped with a magnetic stir-bar. After drying, the flask was cooled to room temperature, the vacuum was replaced with a dried nitrogen atmosphere and PEG was dissolved with 80-mL anhydrous toluene. Next, TEA (34 mmol) was added and AC (20 mmol) in 20-mL anhydrous toluene was dropped wise to the flask at 0 °C with vigorous stirring. Subsequently, the flask was placed in a 45 °C oil-bath and continued for 8 h. The reaction solution was filtered (2C 100 circles; Toyo Roshi Kaisha, Japan) and precipitated in an excess of diethyl ether. The precipitated 4-arm PEG-A was filtered and dried under vacuum at room temperature for 48 h. The final yield was approximately 90%. The acrylation of 4-arm PEG-A, calculated from the ^{1}H NMR spectrum, was 96%.

Synthesis of PEG(-PAE)$_4$ block copolymers

The PEG(-PAE)$_4$ block copolymers were synthesized by Michael-addition polymerization between the vinyl groups at the ends of 4-arm PEG-A, HDDA, and the hydrogens of the secondary amine groups of TMDP (Scheme 1). The general processing to synthesize copolymer P10-03 (Table 1) was as follows: 4-arm PEG-A (0.1 mmol, M_n~10,000) was dissolved in 50-mL DCM at ambient temperature in a 250-mL one-neck round-bottom flask equipped with a magnetic stir-bar. HDDA (6.75 mmol) and TMDP (7.15 mmol) were added and the flask was placed in a 50 °C oil-bath under reflux for 3 days. Finally, the polymer was purified as reported elsewhere [11, 12]. Briefly, the mixture was evaporated under vacuum at 40 °C to remove DCM and dissolving the dried residue dissolved in THF. The copoly-

Table 1 Characteristics of the synthesized the PEG(-PAE)$_4$ copolymers

Number	PEG[a]	PEG(-PAE)$_4$ copolymers				
		M_n[b]	PDI[b]	PAE/arm[b]	PAE[b]	PAE[c]
P2-01	2,000	15,500	1.42	3,375	13,500	13,200
P10-01	10,000	16,100	1.36	1,525	6,100	5,900
P10-02	10,000	18,900	1.32	2,225	8,900	8,500
P10-03	10,000	23,300	1.31	3,325	13,300	13,000

[a] Provided by ID Biochem, Inc.

[b] Measured and calculated from GPC

[c] Calculated from ^{1}H NMR

mer solution was filtered through filter paper (5C 100 circles; Toyo Roshi Kaisha, Japan) to remove the PAE homo-polymer. The THF was then removed at 50 °C under vacuum and the dried copolymer was dissolved in DCM and further purified by precipitating in excess diethyl ether. The precipitated copolymer was filtered and dried under vacuum at room temperature for 48 h. The final yield was approximately 70%. The copolymers of different molecular

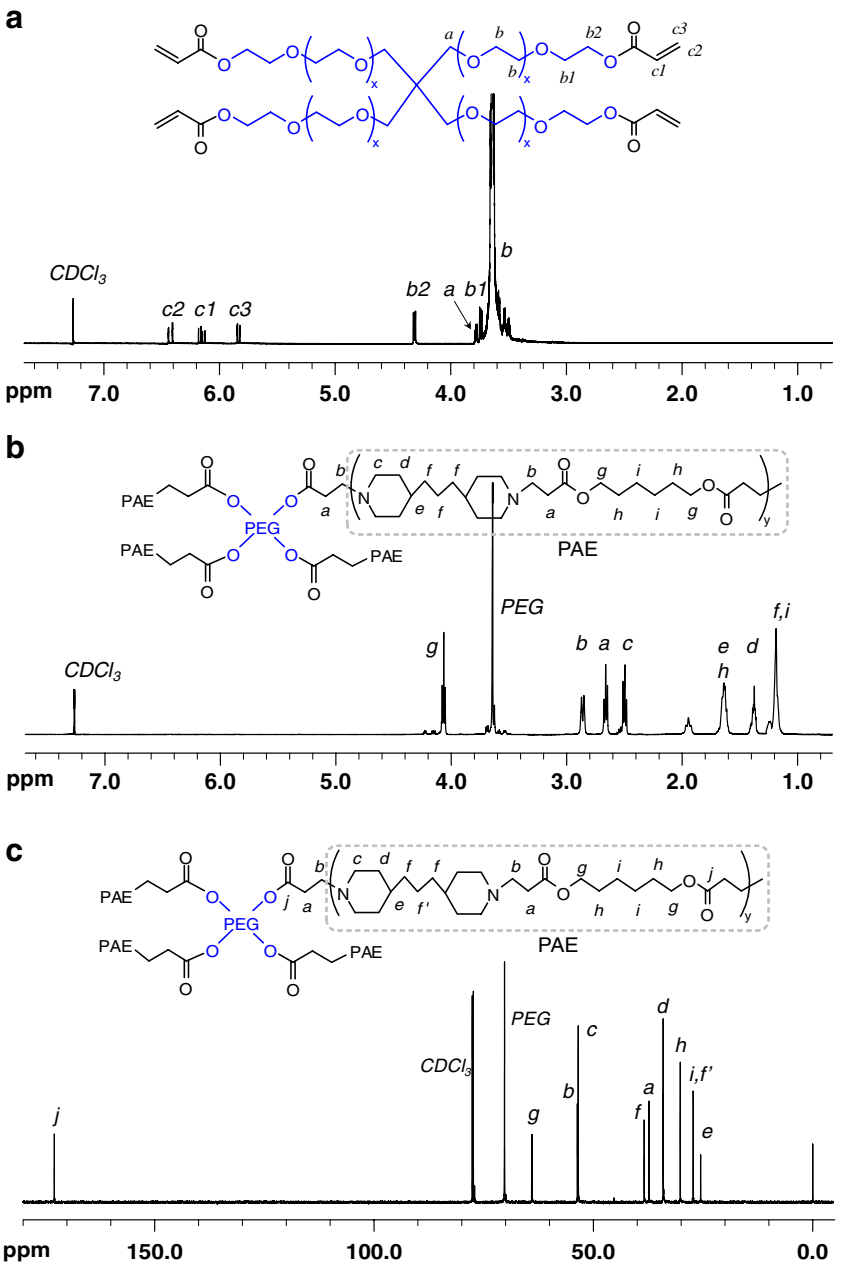

Fig. 1 ^{1}H NMR spectra of 4-arm PEG-A (PEG M_n=10,000) (**a**), PEG(-PAE)$_4$ copolymer (P10-03) (**b**) and ^{13}C NMR spectrum of the PEG (-PAE)$_4$ copolymer (P10-03) (**c**)

weights could be obtained by changing the feed ratio of the reactants and PEG molecular weight.

Characterization

^{1}H and ^{13}C NMR spectroscopy was carried out using a 500 MHz spectrometer (Varian Unity Inova 500NB instrument) to examine the structures of the copolymers in $CDCl_3$.

The molecular weights of the copolymers and their distributions were measured by GPC using a Waters Model 410 instrument with a refractive index detector (Shodex, RI-101) and two Styragel (KF-803 and KF-802.5) columns in series, at a flow rate of 1.0 mL/min (eluent: THF; 40 °C). Poly (ethylene glycol) standards (waters) were used for calibration.

Sol–gel phase transition measurement

The sol (flow)-gel (non-flow) phase transition of the copolymer in an aqueous solution was determined using the tube inverting method. Briefly, the copolymer was dissolved in PBS at pH 1 in a 4-mL vial (10 mm diameter) at a given concentration for 4 h. The pH was then adjusted with 5 N NaOH and 5 N HCl at 0 °C and stabilized at 2 °C overnight. Each vial contained approximately 0.5 mL of the copolymer solution. The sample vials were placed in a water-bath and heated slowly from 0 to 50 °C. The samples were equilibrated for 10 min at temperature intervals of 2 °C [12, 17]. The sol–gel transition was determined by inverting the vial [26].

Rheological properties

The viscosity variation of the copolymer aqueous solutions was determined by dynamic mechanical analysis (Bohlin Rotational Rheometer) [26]. A copolymer solution in PBS was placed between a 20- and 100-mm diameter plate with a gap of 250 μm. Oscillation mode with a stress controlled of 0.4 Pa and frequency of 1 rad/s was performed. The heating rate was 1 °C/min.

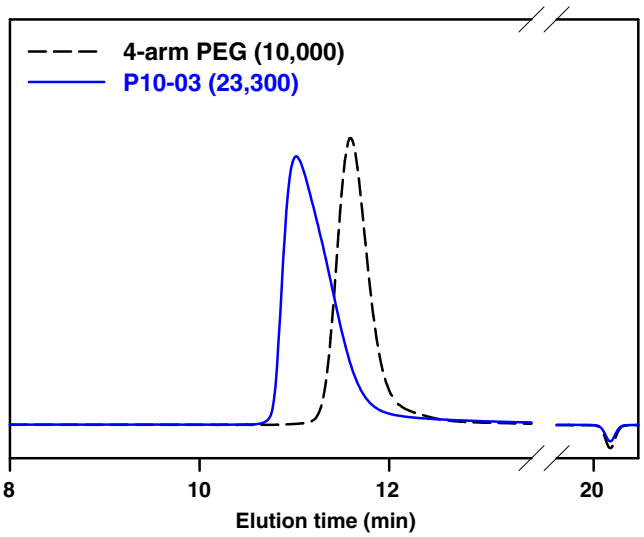

Fig. 2 GPC traces of 4-arm PEG (M_n=10,000) and PEG(-PAE)$_4$ (P10-03)

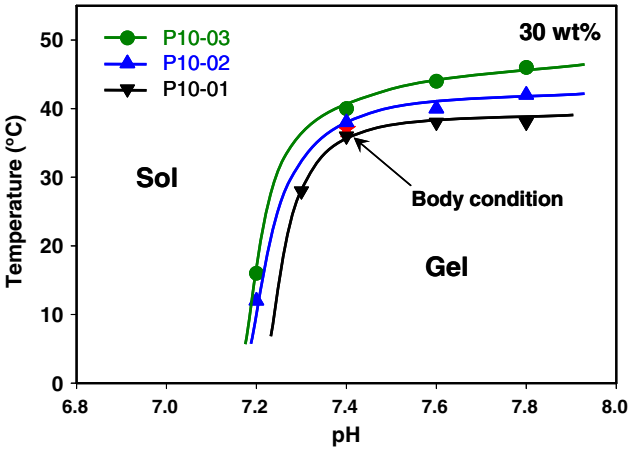

Fig. 3 Sol–gel phase transition diagram of PEG(-PAE)$_4$ copolymer hydrogels (30 wt.%) with different PAE block lengths

In vivo gel formation, gel stability, and gel degradation

Male Sprague–Dawley (SD) rats (Hanlim Experimental Animal Laboratory, Seoul, Korea) were used to study the gel integrity of the aqueous copolymer solutions, gel stability and gel degradation in vivo. The rats (5–6 weeks old, average body weight 200 g) were handled in accordance with the National Institutes of Health (NIH) guidelines for the care and use of laboratory animals (NIH publication 85–23, revised 1985) [26].

An aqueous solution (200 μL, 30 wt.%) of PEG(-PAE)$_4$ copolymer (P10-03) at pH 6.8 was subcutaneously injected into the back of male SD rats to examine the injectability, in vivo gelation, gel stability, and gel degradation. After the designed time, the rats were sacrificed and the gel morphology was observed [13]. The gels were collected and freeze-dried to obtain the residue weight. The remaining weight of the degraded gels in the dry state was calculated by the ratio of lyophilized degraded gels to initial gels. The in vivo gel degradation experiment was examined in triplicate.

Results and discussion

Synthesis and characterization of PEG(-PAE)$_4$ copolymers

Biodegradable star-shaped PEG(-PAE)$_4$ copolymer hydrogels were synthesized by Michael-addition polymerization of 4-arm PEG-A, TMDP, and HDDA in DCM, as shown in Scheme 1. The feed ratio of the reactants and PEG molecular weight were used to control the molecular weight

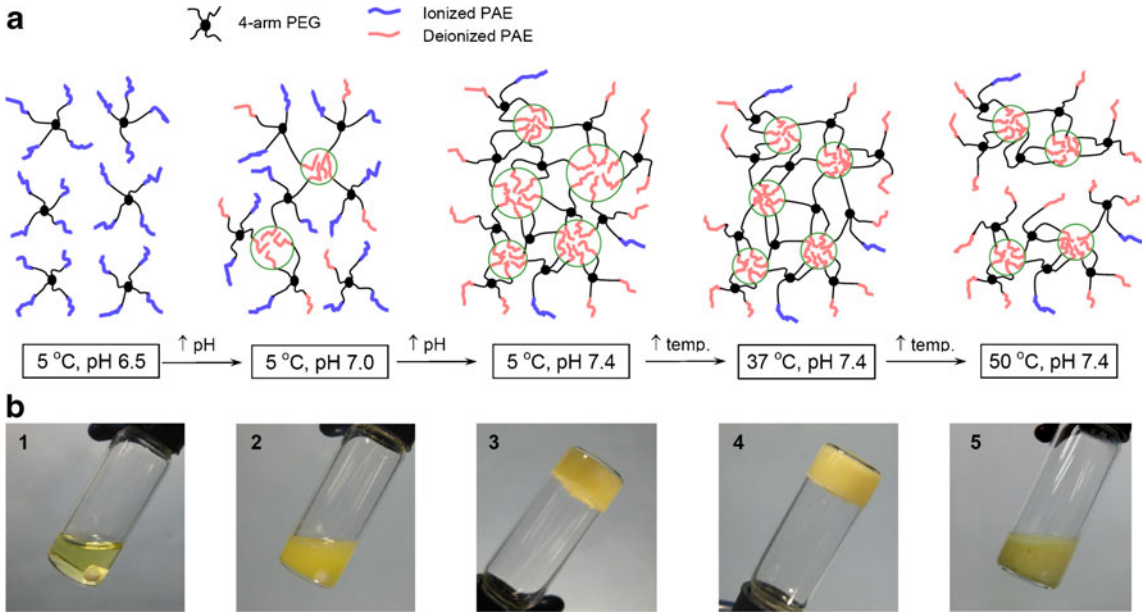

Fig. 4 Schematic showing the sol–gel phase transition (**a**) and in vitro gelation (**b**) of PEG(-PAE)$_4$ copolymer (30 wt.%, P10-03)

of the synthesized copolymers. The formation of 4-arm PEG-A and copolymers was confirmed by ^{1}H and ^{13}C NMR spectroscopy. Figure 1a and b show the proton NMR signals of 4-arm PEG-A and PEG(-PAE)$_4$ copolymer, respectively. As shown in Fig. 1a, the protons at 3.55–3.82 ppm (peaks a, b, and b1), 4.28–4.35 ppm (peak b2) and 5.81–6.49 ppm (peaks c1, c2, and c3) were assigned to the methylene group of PEG, the methylene group at the ends of PEG and the proton in the double bond of AC, respectively, confirming the conjugation of AC to 4-arm PEG. The acrylation yield was 96%, which was calculated from the relatively peaks area of peaks c2 (AC) and b2 (PEG) in Fig. 1a. In Fig. 1b, the protons at 2.88 ppm (peak b) and 2.68 ppm (peak a) were assigned to the methylene protons of the new bond in the copolymer, which were produced by the reaction between the amine groups of TMDP and the vinyl groups of 4-arm PEG-A and HDDA. The peaks of the double bond (5.81–6.49 ppm) disappeared, demonstrating that HDDA and 4-arm PEG-A had been consumed. The protons at 4.06–4.12 ppm (peak g) were assigned to the first methylene of HDDA, indicating the presence of HDDA in the copolymer.

In addition, ^{13}C NMR was used to confirm the structure of the synthesized copolymer (Fig. 1c). As shown in Fig. 1c, the signals at 37.5 ppm (peak a) and 53.9 ppm (peak b) confirmed the formation of the new methylene group. The signals at 70.5 ppm and 64.3 ppm (peak g) were assigned to PEG and the first carbon of HDDA, respectively, demonstrating the formation of a copolymer structure. The molecular weight of PAE blocks was calculated from the ^{1}H NMR spectra with the relatively peaks area of peak g and peak PEG in Fig. 1b and are listed in Table 1. Furthermore, the molecular weights of the copolymers and

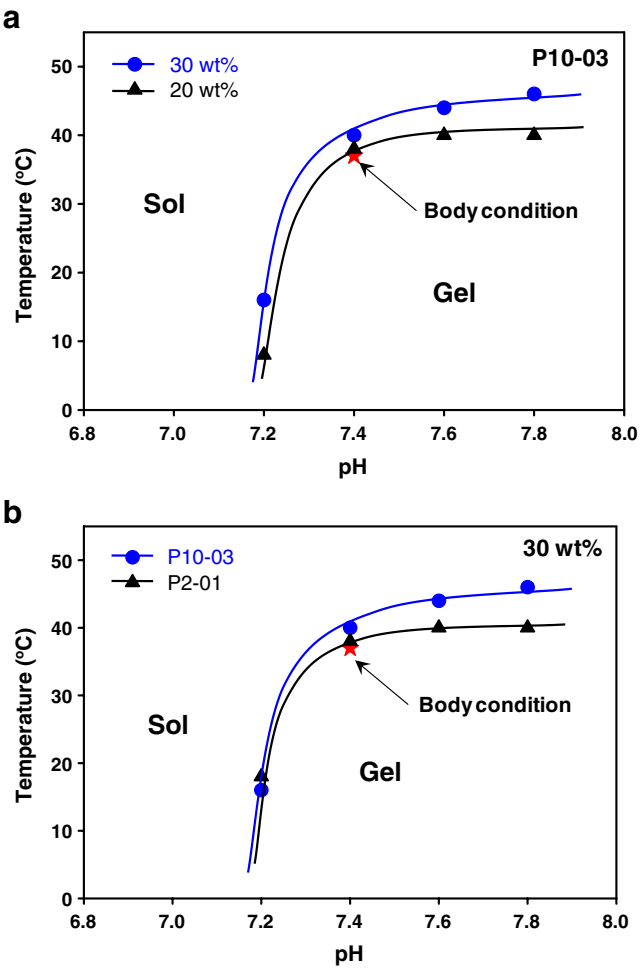

Fig. 5 Sol–gel phase transition diagram of PEG(-PAE)$_4$ copolymer hydrogels with the influence of copolymer concentration (P10-03) (**a**) and PEG molecular weight (30 wt.%) (**b**)

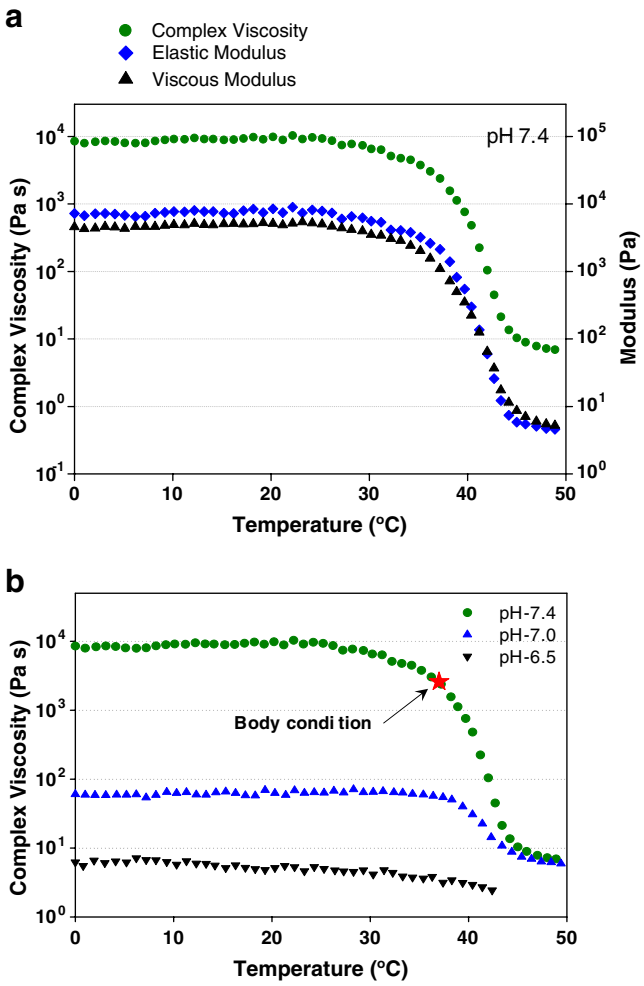

Fig. 6 Rheological properties of 30 wt.% PEG(-PAE)$_4$ copolymer aqueous solution (P10-03) at pH 7.4 (**a**) and different pH values (**b**)

their distributions were determined by GPC. Figure 2 showed the GPC traces of 4-arm PEG (M_n=10,000) and PEG(-PAE)$_4$ copolymer (P10-03). The molecular weights of the copolymers obtained from GPC were similar to those calculated from ^{1}H NMR, demonstrating the formation of a 4-arm star-shaped structure PEG(-PAE)$_4$. The above characterizations clearly indicate the successful synthesis of the PEG(-PAE)$_4$ copolymers. Table 1 lists the characteristics of the synthesized copolymers.

Sol–gel phase transition diagram of PEG(-PAE)$_4$ copolymers

The sol–gel phase transitions of the PEG(-PAE)$_4$ copolymers in aqueous solutions were measured using the tube inverting method under various pH and temperature. In solution, the PAE blocks act as pH/temperature-sensitive blocks [11, 20, 26]. Figure 3 shows the sol–gel phase transition of the copolymers (P10-01, P10-02, and P10-03) with different PAE block lengths. The copolymers solutions showed a gel-to-sol transition at pH 7.2–7.8. At low pH (such as pH 6.5), the tertiary amine groups in PAE were ionized and the ionized PAE blocks were hydrophilic [11, 26]. Therefore, the copolymer solution existed as a sol in the range of experiment temperatures (0–50 °C). However, the copolymer solutions showed different behavior at higher pH (such as pH 7.4). The PAE blocks were deionized and became more hydrophobic, and the hydrophobic interactions between the deionized PAE blocks led to the formation of microscopic domains [26]. The microscopic domains expanded rapidly with the contribution of 4-arm PEG bridges, resulting in a gel phase.

A schematic diagram of the sol–gel mechanism of PEG(-PAE)$_4$ copolymer hydrogels was depicted in Fig. 4a and the in vitro gelation upon the change of pH and temperature are shown in Fig. 4b. A clear solution, as shown in Fig. 4b1, existed at low temperatures and low pH (such as 5 °C and pH 6.5), due to the hydrophilic properties of the ionized PAE blocks. At low temperature and neutral pH (such as 5 °C and pH 7.0), PAE blocks were partly deionized and microscopic domains formed via hydrophobic interactions between the deionized PAE blocks. However, the small size of the microscopic domains and the weak hydrophobic interaction tended to the form a viscous turbid solution, as shown in Fig. 4b2, instead of a gel. At low temperature and basic pH (such as 5 °C and pH 7.4), the PAE blocks were completely deionized and the microscopic domain rapidly expanded, resulting in a turbid gel as shown in Fig. 4b3 [26]. At the constant basic pH (such as pH 7.4), the gel state occurred originally at low temperature (5 °C). When the temperature was increased to 37 °C (physiological condition), the microscopic domains showed more packaged and the gel state was maintained, as show in Fig. 4b4 (a turbid gel similar to the gel at low temperature). With further increasing temperature, the gel-to-sol transition happened (a turbid solution at 50 °C as shown in Fig. 4b5) because of the partial dehydration of PEG and the collapse of packaged microscopic domains at high temperatures [11].

In addition, the effect of the PAE block length, copolymer concentration and PEG molecular weight on the sol–gel phase diagram of PEG(-PAE)$_4$ copolymers solution was examined. Figure 3 shows the influence of the different PAE block lengths on the gel region. With increasing PAE block length from 1,525 to 2,225 to 3,325 (P10-01 to P10-02 to P10-03, respectively), the gel region became wider and shifted to a lower pH due to the stronger interactions between the longer hydrophobic PAE blocks [11, 26]. The gel region at higher pH (pH 7.8) was wider than that at a lower pH (pH 7.2) because of the extended deionization of PAE blocks. Figure 5 shows the effect of the copolymer concentration and PEG molecular weight on the sol–gel phase diagram of the copolymer solutions. As shown in Fig. 5a, the gel window became wider and shifted

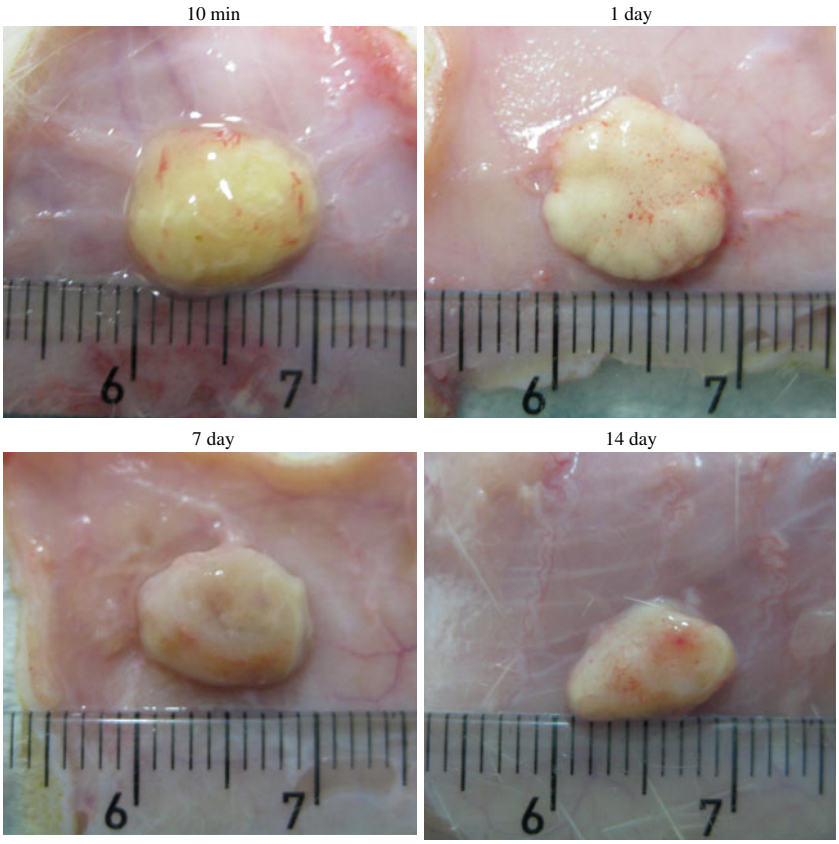

Fig. 7 Photograph of the in situ gel formation and the in vivo gels stability at different period of time after being injected subcutaneously into the SD rats (30 wt.%, pH 6.8, P10-03)

to a lower pH when the copolymer concentration was increased from 20 to 30 wt.% because of the high density microscopic domain, increase in the number of hydrophobic interactions and increase in 4-arm PEG bridges [11, 26]. Figure 5b shows the effect of the PEG molecular weight on the sol–gel phase diagram. At the fixed PAE molecular weight ~3,350, the gel-to-sol transition temperature fell from 40 to 38 °C (at pH 7.4) when the PEG molecular weight was decreased from 10,000 to 2,000. This was explained by a decrease in the ratio of hydrophobic (PAE) to hydrophilic blocks with increasing PEG molecular weight [11]. Moreover, the flexibility of deionized PAE was limited with the short chain of PEG, resulting in deformation of the microscopic domains.

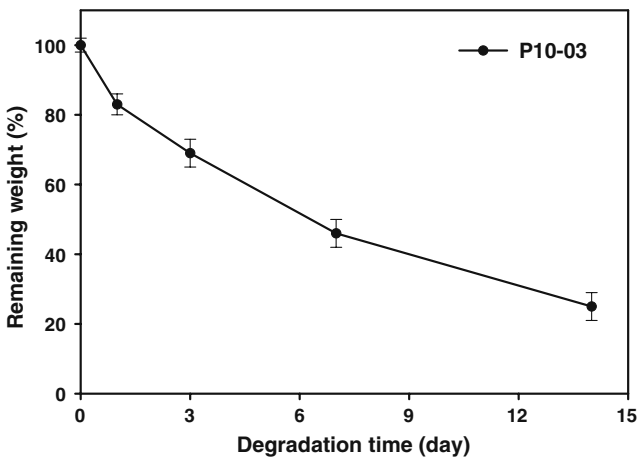

Fig. 8 In vivo degradation of hydrogel P10-03 (30 wt.%) obtained by mass loss method (n=3)

Rheological properties

Dynamic rheological analysis was used to confirm the sol–gel phase transition of the copolymers in solution. Figure 6a shows the change in complex viscosity, elastic modulus (G') and viscous modulus (G'') of the copolymer solution (30 wt.%, P10-03) with temperature at pH 7.4. The copolymer solution exhibited high viscosity (~10^4 Pa s), and $G'>G''$ at 0–41 °C, indicating that the copolymer solution existed in the gel state. At 41 °C, the viscosity decreased rapidly due to the dehydration of PEG at high temperatures [11], and the copolymer solution changed to a sol state ($G''>G'$). This behavior confirmed the gel-to-sol transition temperature, which was determined using the tube inverting method (40 °C). In addition, the viscosity of the copolymer solutions (P10-03, 30 wt.%) at different pH was investigated. As shown in Fig. 6b, at the pH 6.5, the sample viscosity was low (<10 Pa s), indicated the existing of the sol state. At the pH 7.0, the viscosity showed a higher value (~60 Pa s) but $G''>G'$ in the range

of temperatures 0–50 °C, demonstrating the sol state of copolymer solution (viscous and turbid solution as shown in Fig. 4b2). At pH 7.4, the viscosity was high (~10^4 Pa s) and $G'>G''$ at 0–41 °C, indicating a gel state. This result indicates the effect of pH on the sol–gel transition diagram.

In vivo gel formation, gel stability and gel degradation

The copolymer solution (200 μL, 30 wt.% P10-03, pH 6.8, and 20 °C) were subcutaneously injected into the back of male SD rats to examine the injectability, the in vivo gelation of the aqueous copolymer solution and the in vivo stability and degradation of the gel. At a designed time, the rats were sacrificed and the morphology of the gel was observed. The pH 6.8 was selected to inject because of its suitable viscosity to inject and prevent needle clogging. At the higher pH (such as pH 7.0), the viscosity is rather high (~60 Pa s, Fig. 6b) and it is difficult to inject. After the copolymer solution was injected, the outer layer of the gel can reach the equilibrium state immediately and cover outside the gel. The followed step, equilibrium state occurring entire the gel, can be reached in a short time (1–2 min). As shown in Fig. 7, a light saffron gel formed in situ in a short time after injection as a result of the chances in pH and temperature caused by the body conditions of the rats. The gel maintained inside the rats for more than 2 weeks with the decrease in size (Fig. 7). The decrement of gel size can be explained by the degradation of the copolymer and erosion of by-products. Poly(β-amino ester) is a well-known biodegradable polymer with a rather fast degradation rate because of the abundant ester group inside [12, 17, 27]. In addition, the in vivo degradation of P10-03 gels obtained by mass loss method is shown in Fig. 8. The remaining weight of the gels decreased with increase degradation time, confirming that the degradation of copolymer and erosion of by-products caused the gel size decrement. This result suggests that the copolymer solution can be easily injected into the body and the gel can form rapidly. The formed gel could maintain inside the body for a long period of time. Therefore, this copolymer can be a potential carrier for sustained release of drugs/proteins.

Conclusions

A series of biodegradable star-shaped PEG(-PAE)$_4$ pH/temperature-sensitive hydrogels was synthesized and characterized. The copolymer aqueous solutions exhibited a gel-to-sol phase transition as a function of temperature in the pH range 7.2–7.8. The gel window covers the physiological conditions (37 °C and pH 7.4) and can be controlled by varying the PAE block length, copolymer concentration and PEG molecular weight. After a subcutaneous injection of the copolymer solution into the SD rats, the gel was formed in situ within a short time and the formed gel remained for more than 2 weeks in the rat body. This copolymer is expected to be a potential candidate for biomedical applications.

Acknowledgments This work was supported by Basic Science Research Program through the National Research Foundation of Korea (NRF) grant funded by the Korean government (MEST) (2010-0027955).

References

1. Hoffman AS (2002) Adv Drug Delivery Rev 53:3
2. Nguyen MK, Lee DS (2010) Macromol Biosci 10:563
3. He C, Kim SW, Lee DS (2008) J Controlled Release 127:189
4. Jeong B, Bae YH, Lee DS, Kim SW (1997) Nature 388:860
5. Shim MS, Lee HT, Shim WS, Park IS, Lee HJ, Chang TH, Kim SW, Lee DS (2002) J Biomed Mater Res 61:188
6. Yu L, Zhang H, Ding J (2010) Colloid Polym Sci 288:1151
7. Bae SJ, Joo MK, Jeong Y, Kim SW, Lee W, Sohn YS, Jeong B (2006) Macromolecules 39:4873
8. Guiney LM, Agnello AD, Thomas JC, Takatori K, Flynn NT (2009) Colloid Polym Sci 287:601
9. Janovak L, Varga J, Kemeny L, Dekany I (2008) Colloid Polym Sci 286:1575
10. Chun C, Lee SM, Kim SY, Yang HK, Song S (2009) Biomaterials 30:2349
11. Nguyen MK, Huynh CT, Lee DS (2009) Polymer 50:5205
12. Huynh DP, Nguyen MK, Pi BS, Kim MS, Chae SY, Lee KC, Kim BS, Kim SW, Lee DS (2008) Biomaterials 29:2527
13. Huynh DP, Im GJ, Chae SY, Lee KC, Lee DS (2009) J Controlled Release 137:20
14. Nguyen MK, Park DK, Lee DS (2009) Biomacromolecules 10:728
15. Nguyen MK, Lee DS (2010) Macromol Res 18:284
16. Nguyen MK, Lee DS (2010) Chem Comm 46:3583
17. Huynh DP, Nguyen MK, Kim BS, Lee DS (2009) Polymer 50:2565
18. Huynh DP, Nguyen MK, Lee DS (2010) Macromol Res 18:192
19. Tran NQ, Joung YK, Lih E, Park KM, Park KD (2010) Biomacromolecules 11:617
20. Dayananda K, He C, Park DK, Park TG, Lee DS (2008) Polymer 49:4968
21. Futami J, Kitazoe M, Maeda T, Nukui E, Sakaguchi M, Kosaka J et al (2005) J Biosci Bioeng 99:95
22. Kim SH, Jeong JH, Joe CO, Park TG (2005) J Controlled Release 103:625
23. Choi YK, Bae YH, Kim SW (1998) Macromolecules 31:8766
24. Hiemstra C, Zhong Z, Li L, Dijkstra PJ, Feijen J (2006) Biomacromolecules 7:2790
25. Nagahama K, Ouchi T, Ohya Y (2008) Adv Fuct Mater 18:1220
26. Huynh CT, Nguyen MK, Huynh DP, Kim SW, Lee DS (2010) Polymer 51:3843
27. Lynn DM, Langer R (2000) J Am Chem Soc 122:10761